Fracture of the Interlayer Junction of the Shell from a Deep-sea Hydrothermal Vent Gastropod

by

Kevin Wheeler

SUBMITTED TO THE DEPARTMENT OF MATERIALS SCIENCE AND ENGINEERING IN PARTIAL FULFILLMENT OF THE REQUIREMENTS FOR THE DEGREE OF

BACHELOR OF SCIENCE
AT THE
MASSACHUSETTS INSTITUTE OF TECHNOLOGY

MAY 2008

Signature of Author _____
Department of Materials Science and Engineering
May 9, 2008

Certified by _____
Christine Ortiz
Professor of Materials Science and Engineering
Thesis Supervisor

Accepted by _____
Caroline A. Ross
Professor of Materials Science and Engineering
Chair, Undergraduate Thesis Committee

Acknowledgments

I would like to thank Professor Ortiz's group namely Haimin Yao and Juha Song – Haimin, for helping me get coordinated with lab training, access, background materials, sample preparation, and helping me understand several aspects of the project and the materials I worked with. Juha Song, for assisting me with all of the microscopy and microindentation experiments that were performed including organizing the data and reviewing the background material. I also want to thank Professor Christine Ortiz for giving me the opportunity to participate in this very exciting and cutting-edge research group as her thesis advisee. Finally, I'd like to thank the ISN and DMSE, for the use of their labs and providing me with a great learning experience as an undergraduate working on my thesis.

Indirect funding sources for this project may have included:

Institute of Soldier Nanotechnology

Fracture of the Interlayer Junction of the Shell from a Deep-sea Hydrothermal Vent Gastropod

by

Kevin Wheeler

Submitted to the Department of Materials Science and Engineering on May 9, 2008 in Partial Fulfillment of the Requirements for the degree of Bachelor of Science in Materials Science and Engineering.

Abstract

There is considerable amount of interest in the hierarchical nanomechanical processes that contribute to property amplification of biomaterials. An investigation of these processes and the quantification of the mechanical properties and structure of a biomaterial multilayer is determined. The multilayer was composed of an inner, aragonite-like layer and a middle, compliant layer with a gradient layer between the two exhibiting a non-uniform composition and structure. It was found that the hardness of the middle, compliant layer was 0.186±0.007 GPa, while the inner, aragonite-like had a hardness of 2.1±0.22 GPa. The hardness was found to be 1.66±0.44 GPa within the gradient layer. The indentation toughness of the inner layer was found to be 0.307±0.097 $MPa*m^{1/2}$. It was also found that cracks propagated along the grain boundaries within the inner and gradient layers. Crack growth was thus driven by the separation of the grains. The formation of multiple cracks ahead of the crack tip suggested the formation of bands analogous to dilatation bands observed in nacre under certain stress-states. Thus, the mechanisms behind grain separation, the micro-architecture of the anisotropic aragonite grains and other constituents, and the gradual compositional change observed in the tougher gradient layer all acted as toughening mechanisms and contributed to overall property amplification of the shell.

Table of Contents

Goal

The goal of this research is to investigate the hierarchical nanomechanical processes of crack propagation at a biomaterial bilayer of a gastropod shell and to quantify the mechanical properties of the shell in addition to understanding how/why these properties change as the distance from the bilayer interface changes. This would be done in an attempt to better understand the energy-dissipating mechanisms behind property amplification the gastropod shells exhibit with respect to strength and toughness.

Motivation

Living organisms have evolved over time to survive within their environments. In this case, a certain type of gastropod within the Neomphalia family found in the Indian Ocean has developed natural body armor to protect themselves from environments with temperatures reaching 400°C containing an abundance of hydrogen sulfide, iron and other minerals. The feet of the gastropod are covered by dermal sclerites which are composed of conchiolin mineralized with pyrite (FeS_2) and greigite (Fe_3S_4). Interestingly, the relatively weak macro mechanical properties of the proteins, calcium carbonate, bioceramics, minerals, etc. which compose the gastropod shell, exhibit property amplification with huge increases in strength and toughness. This is due to complex, hierarchical nanomechanical processes involving energy-dissipating mechanisms not available in synthetic, hard body armor. However, many of these processes are largely unknown. Thus, investigating these processes and properties is essential to understanding design principles for mechanical property amplification. Once understood, synthetic materials could be made to replace current design. This area of research is promising in

making revolutionary changes in the evolution of engineering systems which could potentially be applied to all aspects of nanotechnology and materials science and engineering. This investigation is also promising in the area for biologically-based material replacement.

Background

Before beginning the project, it was essential to understand the structure of the gastropod and its shell that was to be investigated. As Fig. 1 shows, the gastropod shell is composed of two main layers: an inner, brittle layer and a middle, compliant layer.

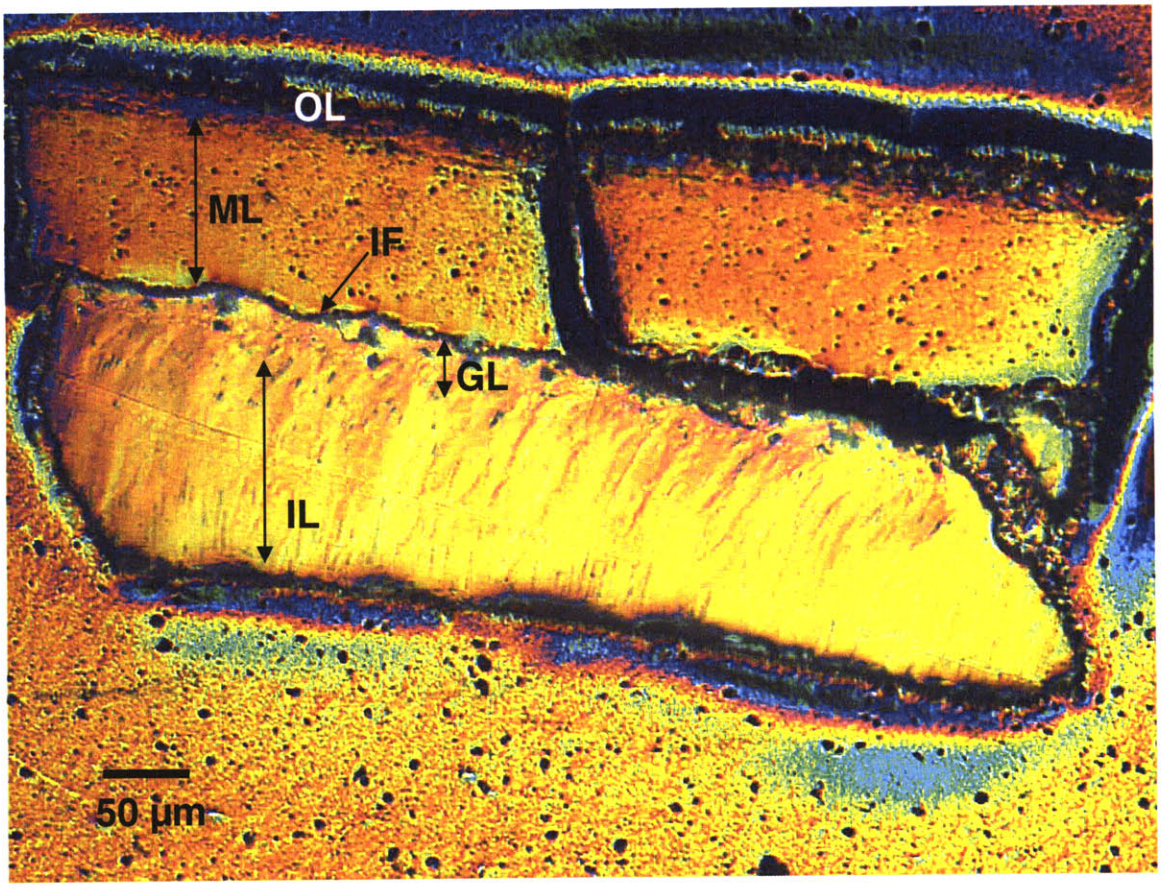

Fig. 1. Optical microscope image taken under crossed-polars of gastropod shell at 100x resolution. As shown, the gastropod shell is comprised of an inner layer (labeled IL), gradient layer (GL), interface (IF), middle layer (ML), and a thin outer layer (OL).

The inner layer is a brittle material with a composition of aragonite (a polymorph of $CaCO_3$) and possibly some other unknown constituents, as shown in Figs. 2 and 3. This inner, aragonite-like layer is about 150-200 μm thick. The middle layer's composition is still largely unknown, but experiments have shown it is composed of organic materials. This layer is about 120-150 μm thick. These two materials are separated by a distinct interface and another distinct region between the inner layer and the interface called the gradient layer. The gradient layer is believed to not be homogenous in composition and structure with respect to the inner layer, and the determination of its properties and crack propagation mechanics was a central focus to this project. Lastly, the gastropod shell has a thin outer layer, about 30 μm thick, composed of some form and/or combination of greigite (Fe_3S_4) and pyrrhotite (Fe_7S_8), as shown from Fig. 2.

It should also be mentioned that one of the very unique features of this gastropod is that its feet are covered by dermal sclerites made of greigite and pyrite (as mentioned earlier). It is speculated that the development of such body armor has evolved to protect the gastropod from not only its harsh environment (dissolved sulfides and minerals with temperatures reaching up to 400°C, but also from potential predators. Specifically, it is speculated that the sclerites protect the gastropod from a predatory gastropod of the genius *Phymorhynchus* which injects venom into its prey (the sclerites are too thick for the venom-carrying radular darts to penetrate)[5]. Additionally, the mineral fortification of the sclerites is directly controlled by the gastropod[5]. This is very unique as the organism is able to manipulate the inorganic compounds incorporated into its own armor. This concept of evolutionary design is fascinating and one of the principle areas of interest in

studying biomaterials like this. It is believed that if we can understand the biological and evolutionary design principles behind biomaterials like this, we could apply this knowledge to replace current engineering and design principles.

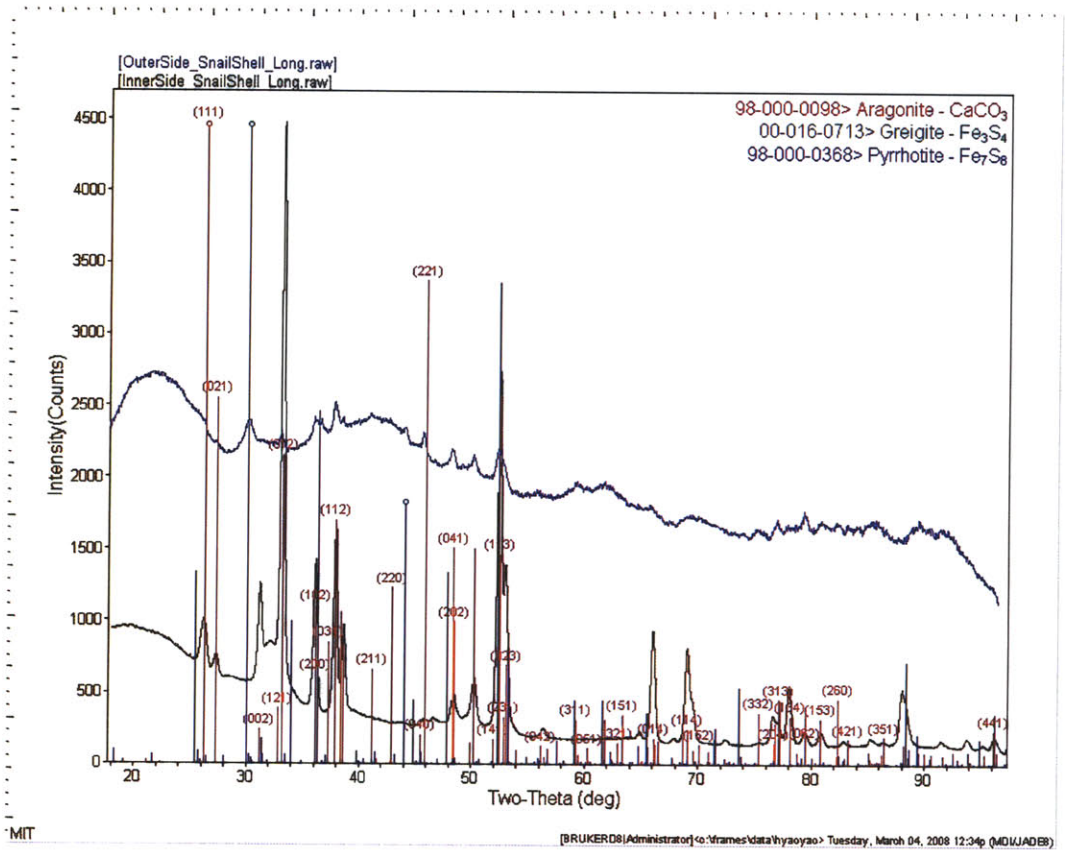

(*experiment and image source: Haimin Yao*)

Fig. 2. X-ray diffraction analysis on the inner (black plot) and outer (blue plot) layers of the gastropod shell. Formatting these plots to known peaks of aragonite ($CaCO_3$), greigite (Fe_3S_4), and pyrrhotite (Fe_7S_8) it can be seen that the outer layer is some form of an iron sulfide while the outer layer appears to closely resemble aragonite with the possibility of some sulfur content.

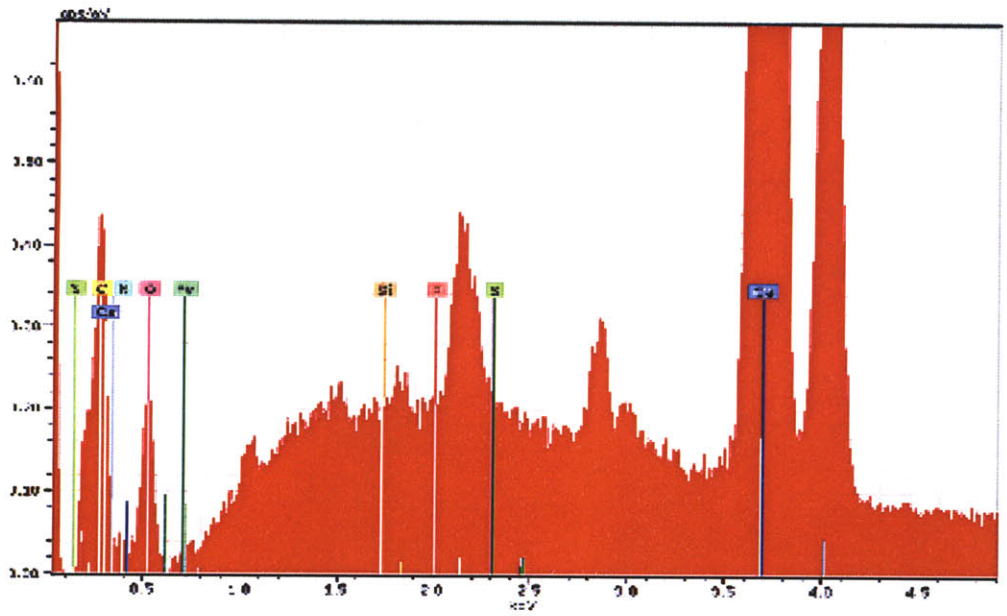

(*experiment and image source: Haimin Yao*)

Fig. 3. Energy dispersive x-ray analysis on the inner layer of the gastropod shell. Formatting these plots to known peaks (from right to left on the image) of Ca, S, P, Si, Fe, O, N, C, Ca, and S, it can be seen that the peaks from the EDX analysis match closely with the Ca, C, and O peaks with another EDX peak between the P and S peaks suggesting sulfur as a possible content as well. This supports the notion that the layer is composed of an aragonite ($CaCO_3$) based material.

Emphasis was focused on studying the interface junction between the middle and inner layers (including the interface and gradient layer), because the middle and inner layers were believed to serve as a primary source for the material's amplified strength and toughness much like human teeth[3]. For instance, human teeth include two distinct regions: an inner, compliant region made of dentin and an outer, brittle region made of enamel. The enamel makes the teeth hard and strong, but its brittleness makes the teeth subject to catastrophic micro-cracks. However, as cracks approach and pass the dentin-enamel interface, they arrest as uncracked bridged fibrils absorb much of the load and energy from the cracks[3]. These processes serve as toughening mechanisms[3]. In the gastropod shell, however, the layers are reversed (the inner layer is brittle and the middle layer in

compliant), and an investigation at the interface junction between the two layers could serve to explain the resulting toughness and strength of the shell.

The gastropod itself is a unique form of mollusk in the sense that its feet are covered by dermal sclerites which are composed of conchiolin mineralized with pyrite (FeS_2) and greigite (Fe_3S_4). These sclerites cover the feet in a roof-tile manner where the outer, mineralized layer is ferromagnetic. The gastropods are found in the Kairei vent field in the Indian Ocean where temperatures can reach up to 400° and the environments are rich in dissolved sulfides and metals. These sclerites are believed to protect the gastropod from both their harsh environments and potential predators.

Project Considerations

The first feature necessary to take into consideration was the amount of time given to fulfill the goals of the project. The project only lasted about 3 months, so it was important to set realistic goals given this time frame at the start. When deciding the goals and expectations, it was important to also take into consideration the amount of time it would take to get trained on the equipment, gain access to the necessary labs, and most importantly to actually prepare the samples and perform the experiments.

That being said, it was also necessary to take into consideration the amount of time it was going to take to learn and understand the background of the project. It was important to understand basic fracture mechanics and crack propagation mechanics of material multilayers and their interfaces in order to understand how the mechanical properties of

the materials affected these mechanisms and how this contributes to the overall amplification of toughness and strength. It was also important to understand the structure of the material as best as possible in order to explain and analyze the results of the experiments.

Another consideration of this project was the scale at which the experiments were going to be performed and the amount of material available for this project. It was necessary to figure out a way to maximize the workable area of the samples given a very limited supply of the material. The material also had to be smooth enough for optical microscopy and SEM to be performed at high resolutions (up to 10,000x). The surface of the samples also had to be smooth enough to actually perform indentation without surface roughness affecting the results.

Pre-experimental Methods

Sample Preparation. Given the limited availability of the gastropod shells, it was very important to find an intact piece that could be prepared for analysis. This meant that a uniform piece of undamaged material whose bilayer was still intact had to be found. This could be done with the naked eye since one can see the interface without the use a microscope (the aragonite-like layer appears white, while the compliant layer appears dark brown/black). Once the sample was prepared, optical microscopy needed to be performed to see if any parts the material and its interface was damaged. The shell is thin and needed to be long and wide enough to be sectioned in large enough pieces that

experiments could be feasibly made. Thus, samples at least about 5 mm in length and 1 mm in width were selected.

Gastropod shell cutting. Once an intact sample was selected, it was necessary to cut the sample into a rectangular shape using a simple razor blade. A razor blade was applied to the top of the surface of the sample and firmly pressed down until the sample broke into the desired section. This was done until a 5 mm x 1 mm sliver was obtained.

Epoxy molding. Once the sample was sectioned, about half of a teaspoon of Loctite Poxy Pak epoxy was dispensed onto a clean piece of aluminum foil. The epoxy was stirred for about 2 minutes using a small, thin rod until the epoxy had a uniform distribution and all bubbles were mixed out. The epoxy solution was then added into a small, rubber molding well about 6 mm long, 4 mm wide, and 3 mm deep. Using tweezers, the gastropod shell sample was evenly placed into the epoxy until the top of the material was completely submerged under the surface of the epoxy. It was ensured that the sample was placed as straightly and evenly as possible so that the top layer was parallel to the surface of the epoxy (and its cross section parallel to side of the well wall). The sample was allowed to sit in the epoxy until the epoxy dried and hardened overnight, embedding the sample in it.

Diamond saw cutting. Using an Isomet diamond saw with Buehler diamond wafering blade (series 15HC diamond), the mould was cut along the cross-section of the gastropod shell sample into slices of about 1.5 mm to 2.0 mm thick. The samples were cut in such a

way that no manual force was applied. This took about 3-5 minutes per slice. This was ensured so that the blade of the saw would not damage the surface of the sample. It was ensured that each slice side was parallel with the other to maximize the cross-section area.

Securing samples. Once slices of the samples embedded in epoxy were cut, each slice was glued to the surface of generic dime-sized discs using generic super glue. It was ensured that the surface that exposed the cross-section of the gastropod shell sample was facing up (parallel to the disc). The samples were allowed to dry overnight.

Sample polishing. Each sample was polished using a Buehler diamond polisher. The speed was set to its minimal point. The grain size of the diamond polishing paper used was 0.1 μm. Water drops were applied at a rate of about 1 drop per second to the polishing wheel during polishing. The samples were placed face-down onto the polisher and polished in 10 minute segments until the sample surface was completely polished.

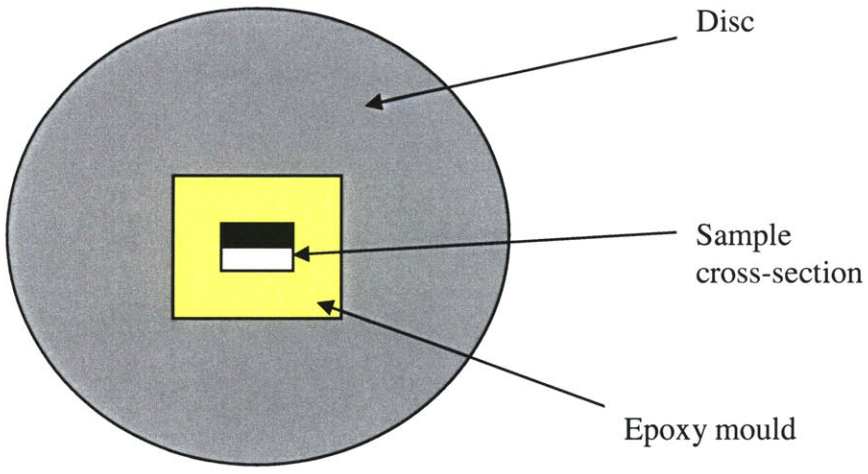

Fig. 4. Top-view of prepared sample. The black and white cross-section represent the middle, compliant layer and the inner, brittle layer respectively.

Experimental Methods

Optical Microscopy before microindentation. Before microindentation was performed, the samples were visually inspected. This was done to ensure the sample was intact and undamaged. Damaged samples could still be workable, but reliable measurements could not be made near the damaged areas. Since a main focus of this project was to analyze the mechanisms of crack propagation at the interface, it was essential that none the interfaces were separated, though many still had cracks along them. It was also ensured that the sample was polished such that surface roughness was eliminated. This was done to ensure reliable and accurate results. Using a Nikon Elipse L150 (Tokyo, Japan) optical microscope, each sample was imaged at resolutions of 25x, 100x, 200x, and 500x. Several images were taken and saved.

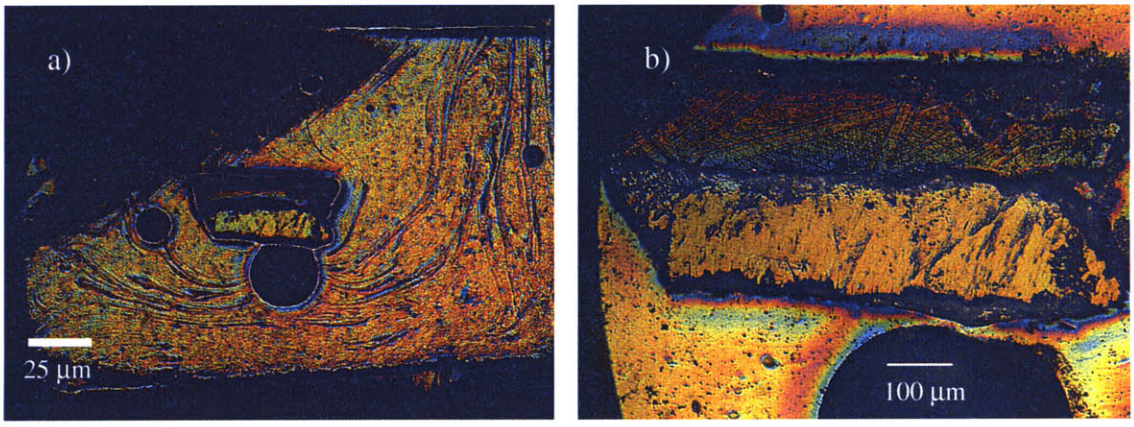

Fig. 5. a) Optical microscope image at 25x. The sample is seen in the middle with a distinct multilayer and interface. The dark circle below the sample is a bubble in the epoxy. The dark region in the upper left is due to surface roughness. **b)** Same image at 100x. One can notice the effect that roughness and bubbles have on the images and on the surface of the sample. The amount of experimentation that could be done was limited due to this.

Optical Microscopy after microindentation. Once microindentation experiments were performed, each sample was again imaged using the optical microscope at resolutions of 25x, 100x, 200x, 500x, and 1000x. It was ensured that the indents and their corresponding cracks (if any) were imaged for later analysis.

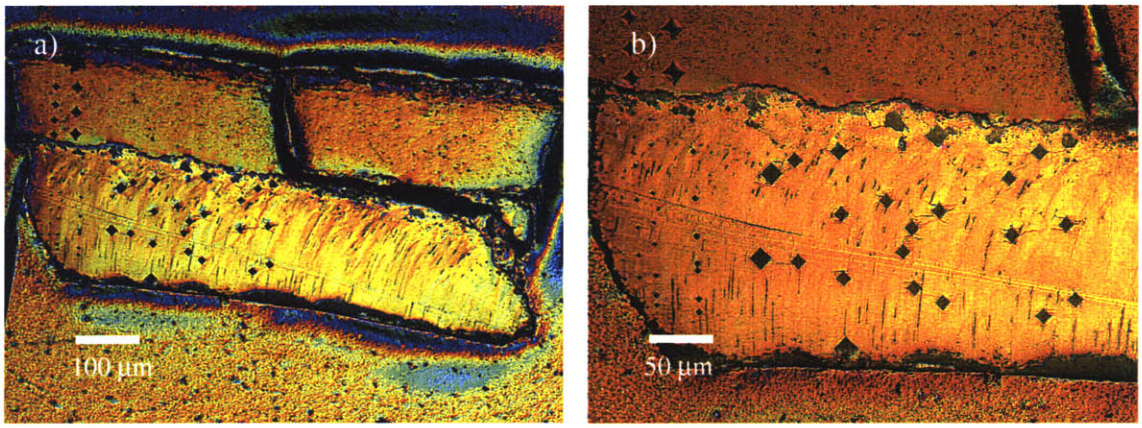

Fig. 6. a) Optical microscope image at 100x. Microindentation has been performed throughout the sample at various loads. Because the right portion of the sample was damaged at the interface, no measurements were made in that region. **b)** Same sample at 200x. Most of the indentation was done in the brittle region where toughness could be measured.

Microindentation. Once the samples were imaged, microindentation was performed on the sample (bilayer cross-section) using a LECO hardness tester (Model LM247AT, LECO Co., St. Joseph, MI, USA). Each sample was placed on the holder and adjusted until it came into focus using the accompanying software. Once the surface of the sample came into focus, areas for indentation were selected. All indents were done using a Vickers hardness indenter.

In order to determine the indentation fracture toughness of the materials, the loads at which the materials fractured, or cracked, needed to be determined as indentation fracture toughness is a function of the residual crack lengths from the indents. Thus, using the relatively most damaged sample (but one which still contains enough intact area for

undisturbed indentation), a load of 5g was applied to each of the two main layers (the inner, aragonite-like layer and the middle, compliant layer). Loads were sequentially increased from 5g to 10g, 50g, 100g, 300g, and 500g until the indents produced a crack. The load that produced fracture was called the critical load.

Once the critical loads were determined, indentation experiments for this method were performed at that load. In order to analyze the mechanisms of crack propagation at and along the interface, indents were made along the interface at distances of about 10-30 μm from the actual interface with inter-indent spacing of about 10-50 μm (depending on the load; the larger the load, the more space between indents was given). This was done along the entirety of the intact, undamaged interface for each sample. In order to determine how (and if) the fracture toughness changes as a function of distance from the interface, indents were also made perpendicular to the interface. Indents were made from the interface to the inner edge of the aragonite-like layer at inter-indent spacing of about 10-50 μm.

In order to determine the hardness values of the sample and how they change as a function of distance from the interface, a similar method was used as described above. In stead of performing indents along (parallel to) the interface, indents were only made perpendicular to the interface from one edge of the sample to the other edge (crossing the interface). Loads of 5g and 10g were employed (both below the critical load). Starting at the inner edge of the aragonite-like layer (adjacent to the epoxy mould), indents were made with inter-indent spacing of about 10-20 μm across the interface and through the

middle, compliant material until the outer edge was reached. Each sequence of indents was done under loads of 5g and10g twice each (a total of 4 sequences as seen in on the left hand side of Fig. 6 where the smaller indents are).

Data analysis and toughness calculations. Once optical microscopy was performed on the indented sample, the images were used to calculate the indentation fracture toughness. Using a micro-ruler, the residual crack lengths from each of the indents equidistant from the interface were measured. The length of a crack was measured from the center of the indent to the end of the crack. Once all crack lengths were determined, the average crack length was determined and the indentation fracture toughness was calculated using,

$$K_{ind,c} = \chi P / c^{3/2} \tag{1}$$

where χ is the residual indentation coefficient, P is the indentation load (in Newtons), and c is the average crack length (in meters)[4,6]. The indentation fracture toughness was then calculated as a function of distance from the interface. The residual indentation coefficient was calculated using the equation,

$$\chi = \underset{V}{\overset{R}{\xi}}(E/H)^{1/2} \tag{2}$$

where χ is the residual indentation coefficient, $\underset{V}{\overset{R}{\xi}}$ is a material-independent constant for Vickers-produced radial cracks (given to be 0.016), E/H is the Young's modulus to hardness[6]. Given H = 5.5 GPa and E = 100 GPa, χ was calculated to be 0.0682.

Hardness calculations. Though the indentation fracture toughness was only calculated for the brittle, inner layer of the sample, the hardness was calculated for the inner, middle, and gradient layers. Using the equation,

$$H_v = 1.854F / d^2 \tag{3}$$

where H_v is the Vickers hardness, F if the load (measured in kgf), and d is the average diagonal length of a residual indent (measured in mm), hardness values were calculated. Multiplying the hardness values by 0.009807 will convert the HV units to GPa. For each hardness value measured, the distance from the center of the indent to the interface was also measured as to compare how the hardness values change with distance to and from the interface. The diagonals were measured from the optical microscope images of only the residual indents that did not cause fracture in the material.

SEM Imaging. Once the above methods were completed, a JEOL JSM 6060 Scanning Electron Microscope (SEM) was used to image the resulting cracks from indentation at much higher resolutions. This was done to actually see and understand how the cracks propagated at the various regions of the sample.

SEM images were taken at resolutions ranging from 1,500x to 9,500x (higher if can get into focus) on various cracks. Specifically, images were taken of cracks approaching the interface and cracks propagating within the bulk part of the inner, aragonite-like layer, as seen in Fig. 7.

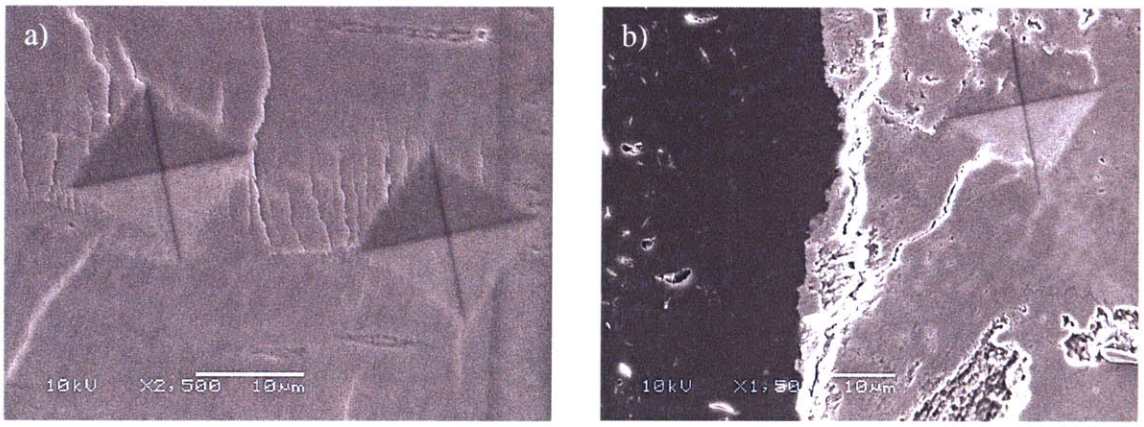

Fig. 7. SEM images. **a)** Image of indents and cracks within bulk part of inner, aragonite-like layer at 2,500x. **b)** Image of indent and crack propagating into crack along interface. The left, darker region is the middle, compliant layer, and the region where the indent is, is the gradient or aragonite-like layer.

Results

During the microindentation, cracks were induced in the brittle aragonite-like layer at loads as low as 50g. Cracks were induced at this load throughout the entire layer up to the interface. Cracks propagated anisotropically from the indents parallel to the interface in the bulk area (distances of more than 35 µm from the interface), as seen in Fig. 8. However, cracks propagated into the interface and arrested at cracks along the interface within the gradient layer (distances up to about 30 µm from the interface), as seen in Fig. 9.

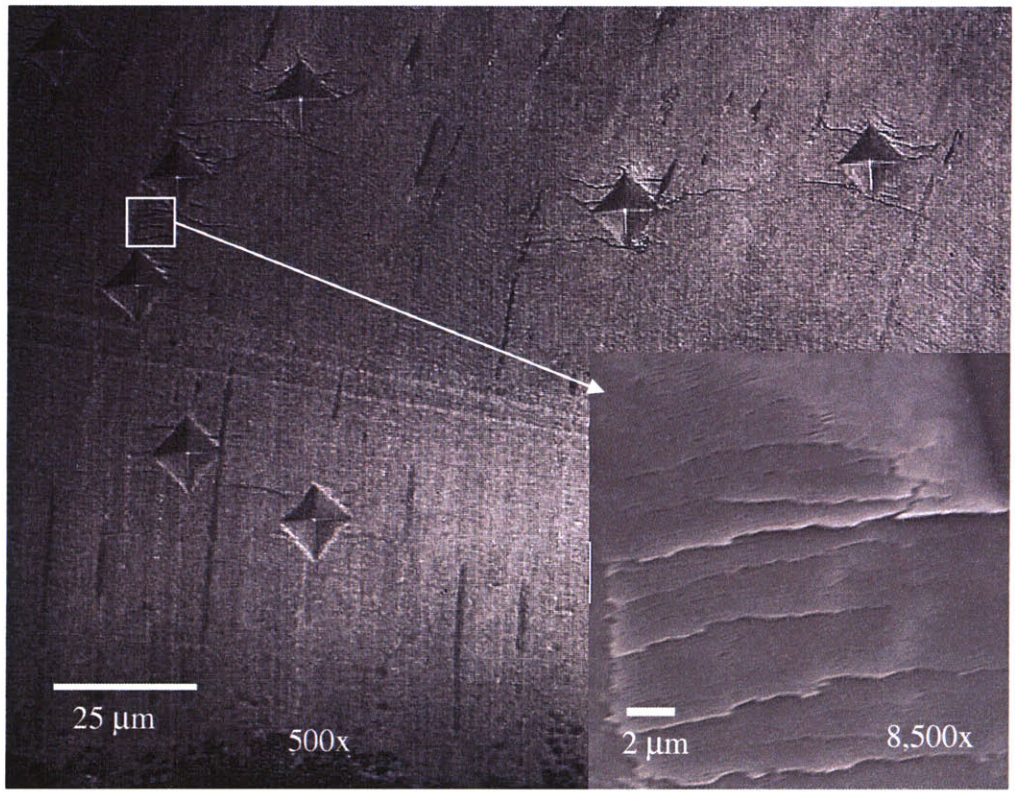

Fig. 8. Optical microscope image of indents of their residual cracks within the bulk region of the inner layer. Inlet more clearly shows the anisotropic nature of crack propagation in this region of the layer.

However, cracks could not be induced to penetrate the bilayer interface. Indents near the interface only induced cracks which propagated along cracks at the interface, but not into the compliant, middle layer.

Direct fracture via indentation could not be induced in the middle, softer, compliant layer at loads up to 300g. Loads higher than 300g were not employed because the residual area of the indents at 300g nearly covered the width of the entire layer. Using equations (1)

and (2), the indentation fracture toughness and hardness values with respect to distance from the interface were determined, as shown in Fig. 10.

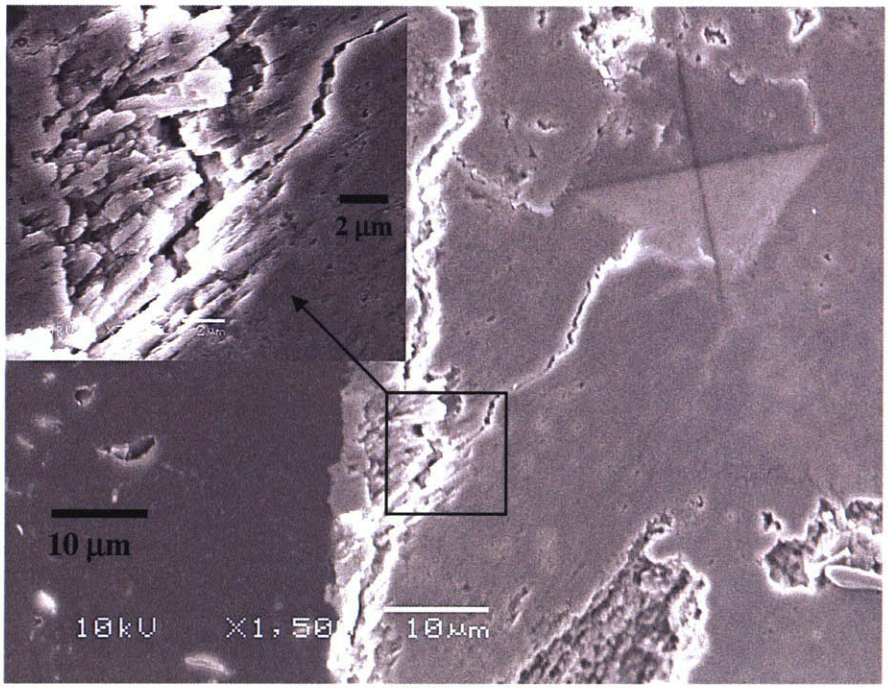

Fig. 9. SEM images of indent and residual crack propagating into interface and arresting at a crack along the interface. Inlet shows the fibril-like nature of the gradient layer structure.

It should also be noted that the number of cracks induced per indent increased as the distance from the interface increased, as roughly seen in Figs. 7 and 8.

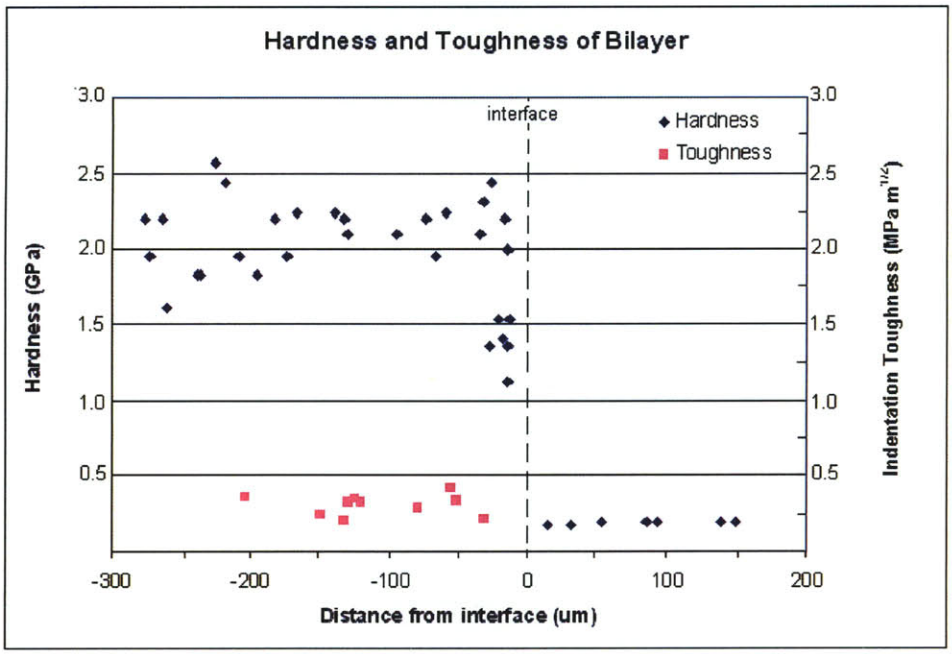

Fig. 10. Profile of Vickers hardness and indentation toughness. Values to the right of the interface line represent those within the middle, compliant layer. Values to the left are within the inner, aragonite-like layer. Hardness values drop off dramatically within 50 μm of the interface and are constant in the compliant layer.

The hardness for the middle, compliant layer was found to be 0.186±0.007 GPa, while it was 2.1±0.22 GPa for the inner, aragonite-like layer. Additionally, the hardness was found to be 1.66±0.44 GPa within the gradient layer. The indentation toughness was found to be 0.307±0.097 MPa*$m^{1/2}$.

Discussion

As Fig. 10 shows, there really was no concrete correlation between fracture toughness and distance from the interface. However, as Fig. 10 also shows, hardness values do change and decrease dramatically as the interface is approached. These results suggest a change in structure and composition as the interface is approached from the inner edge of the inner, aragonite-like layer. But it should be pointed out that these results may have

included some error as they were only based on a limited number of indents, and in some cases, areas of significant surface roughness and interface damage.

The anisotropic nature of crack formation and propagation in the bulk region of the aragonite-like layer also suggest anisotropy with respect to their grains. As seen in Fig. 11, the anisotropic nature of the grain boundaries exhibit aspect ratios much greater than one in a tablet-like nature.

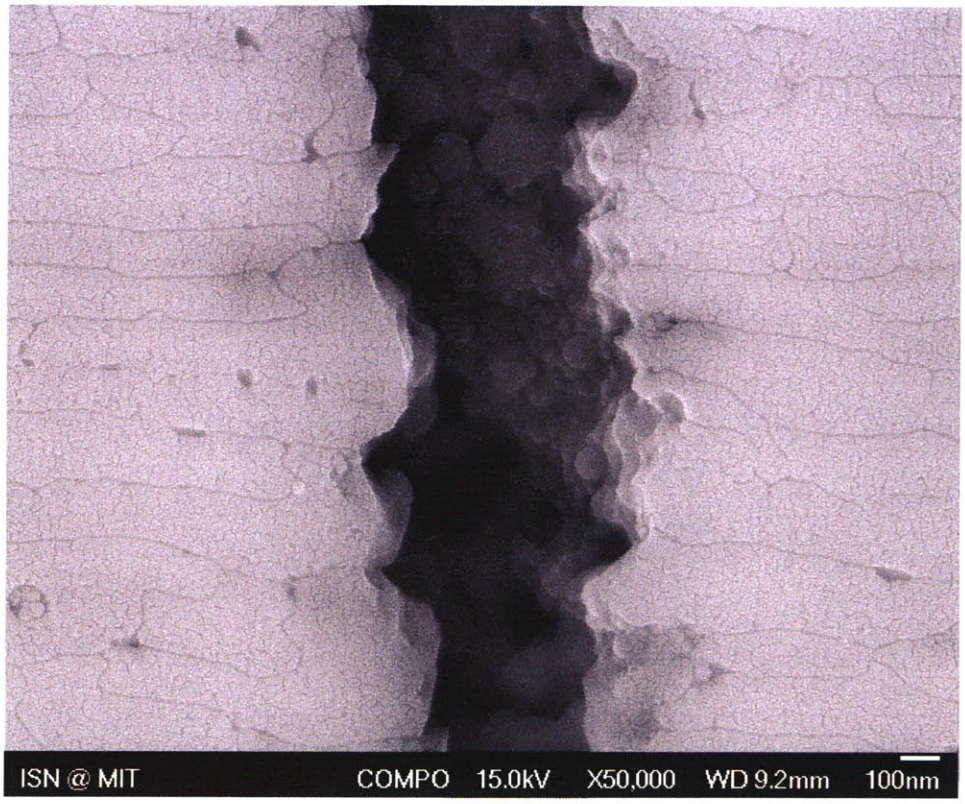

(*image source: Haimin Yao*)

Fig. 11. SEM image of crack in inner, aragonite-like layer. On either side of the crack, it is clear to see individual grains and how they exhibit an anisotropic nature.

As Fig. 9 revealed, the cracks propagated along, rather than through, the grain boundaries. Thus crack propagation was controlled by the separation of these grains. This suggests that work necessary to separate the grains (forming the cracks) acted against the crack

driving force (consumed some of that energy), meaning that this separation mechanisms acted as a toughening mechanisms, inhibiting crack growth. As Fig. 8 also shows, several cracks formed ahead of the crack tip originating from the indent. These cracks resembled "bands" analogous to "dilatation bands" which are apparent in nacre under certain stress-states.[7] The major difference between the bands observed here and those observed in nacre is that they traverse along the length of the grains (along the orientation of the grains) rather than along the width (along the perpendicular direction with respect to the orientation of the grains). Thus, the deformation mechanisms of the material observed here seems to be a combination of dilatation bands and brittle fracture. The appearance of a deformation other than brittle fracture suggest that there might be an additionally constituent other than aragonite within the inner layer helping to hold the grains together (this is talked about in more detail below). Again, these findings are also important as they suggest that the energy necessary for crack propagation is dissipated by the energy required to separate these grains. Thus the separation of grains acts as a toughening mechanism.

It suggested above, the composition of the inner layer may not be entirely aragonite. Previous experiments have shown that aragonite has a fracture toughness of about 0.1-0.2 $MPa*m^{1/2}$, which is 2-3 times lower than the results found in this project[7]. Additionally, XRD and EDX (as seen in Figs. 2 and 3) suggest that the inner layer may have other constituents besides calcium carbonate as evidenced by the unlabeled peaks in both figures. The fact that there are unlabeled peaks also suggest that these constituents are not organic (possibly some other form of mineral). If there are additional constituents within

this layer, the results explained in the previous paragraphs suggest that these constituents may act as a possible "glue" giving rise to a brick-and-mortar structure analogous to nacre (however not nearly as tough or strong as nacre). These constituents could thus also act as toughening mechanisms by absorbing some of the crack propagation driving force (analogous to nanoasperities or mineral bridges)[7]. However, the properties of the inner layer do not mimic those of nacre and the XRD and EDX results, as stated above, do not seem to support the notion that this layer has an organic matrix like nacre (nor that it is organic at all), which suggests that these possible constituents are not nearly as tough as the organic matrix found in nacre and are probably some form of mineralized deposits.

The anisotropic nature of the grains also suggests that crack propagation is much more limited in the direction perpendicular to the orientation of the grains (as it would require much more energy to separate the grains in this direction). This could explain the formation of anisotropic bands seen in Fig. 8.

However these bands are not apparent in the gradient layer, as seen in Fig. 9. Combining this finding with the fact that the hardness changes dramatically overwhelmingly suggest the composition in this region differs from that of the inner layer. The fact that the dilatation bands are not present suggests that the constituents in this region are absorbing the energy which caused the formation of the bands in the inner layer. However, as evidenced by Fig. 9, aragonite grains are still apparent and the cracks still propagate along the grain boundaries (due to the separation of the grains). This suggests that whatever additional or constituent changes present in the gradient layer would be found

between the grains (unless the grains are composed of something in addition or differently from aragonite). Thus it can be inferred that these constituents also act like a relatively weak "glue" holding the grains together and preventing them separating (again, not nearly as strong as the organic matrix found in nacre).

As stated above, the lack of correlation in toughness results could be due to some significant error. The above findings suggest toughness values should also be directional (tougher in the direction in which the aragonite grains are orientated). However, all of the toughness values were averaged, regardless of crack direction. As explained above, the presence of different (or a different concentration of) constituents within the gradient layer compared to the inner layer prevented the formation of dilation bands in the gradient layer. Thus, the gradient layer should, by all qualitative measures, be tougher than the inner layer.

As the interface is approached, it was observed (as seen in Fig. 9) that cracks tended to propagate into (perpendicular to) the interface. As Figs. 9 and 11 show, the grains seem to change orientation. Within the inner layer they are oriented parallel to the interface (Fig. 11), while they are oriented in a more perpendicular direction within the gradient layer (Fig. 9). Thus, this explains why cracks propagated parallel to the interface in the inner layer (as seen in Fig. 8) and into the interface in the gradient layer (as seen in Fig. 9) as crack propagation is driven by the separation of the grains.

Additionally, the relative consistency of the hardness values in the bulk region of the inner layer and the middle, complaint layer suggest composition and structure that is relatively uniform. Thus, the structures and composition seemingly only begin to change within the gradient layer (within about 50 μm of the interface into the inner-layer side of the interface).

Lastly, as Fig. 9 also shows, cracks propagated to the interface, but arrested at a crack running along the interface. This was a major source of error as cracks could not be forced to penetrate the interface and propagate into the middle, compliant layer. This prevented us from investigated mechanisms and processes of crack growth and crack arrest in the middle layer (exactly what role the middle layer plays in fracture of the material).

Conclusion

The hardness and indentation toughness as a function of distance from the interface was determined for the inner and gradient layers, while only the hardness could be determined for the middle, compliant layer. The mechanisms of crack propagation were observed and explained along with the microstructure and potential composition of the inner and gradient layers. It was determined that the combination of a tough, middle layer and brittle, inner layer contribute to the material's overall property amplification along with the contributions of micro- and nano-structure (grain anisotropy, dilatation-like bands, etc.) and the compositions of the inner and gradient layers. Future works will be directed towards determining the composition throughout the entire material, testing materials

without any damage to them, understanding the material's temperature and corrosion resistant properties, eventually synthetically replicating the properties of this material for applications in body armor and engineering systems.

References

1. Christine Ortiz, et al., "Nanomechanical Heterogeneity as a Design Strategy in Natural and Biomimetic Body Armor," *ISN Research Proposal: Project 3.13*, (2006).
2. Yohey Suzuki, et al., "Gastropod shell formation in the hydrothermal-vent scaly-foot gastropod—possible control of iron sulfide biomineralization by the animal," *Earth and Planetary Science Letters* **242** (2006) 39– 50.
3. V. Imbeni, et al., "The dentin-enamel junction and the fracture of human teeth," *Nature Materials* **4** (2005).
4. John W. Hutchinson, et al., "Crack Deflection at an Interface between Dissimilar Elastic Materials," *International Journal of Solids and Structures* **25** (1989) 1053-1067.
5. Anders Waren, et al., "A Hot-Vent Gastropod with Iron Sulfide Dermal Sclerites," *Science* **302** (2003) 1007.
6. G.R. Anstis, et al., "A Critical Evaluation of Indentation Techniques for Measuring Fracture Toughness: I, Direct Measurements," *Journal of American Ceramic Society* **64** (1981) 533-538.
7. Kearney, Cathal. "Mechanical Behavior of Ultrastructural Biocomposites," *Masters of Science Thesis.* Professor Ortiz group. Massachusetts Institute of Technology. (2006).